Chemical Engineering Science 263 (2022) 118131

Contents lists available at ScienceDirect

Chemical Engineering Science

journal homepage: www.elsevier.com/locate/ces

A process systems Engineering approach to analysis of fructose consumption in the liver system and consequences for Non-Alcoholic fatty liver disease

Yunjie Liao [a,b,*], Nathan A. Davies [b], I. David L. Bogle [a]

[a] Centre for Process Systems Engineering, Department of Chemical Engineering, University College London, London, United Kingdom
[b] Institute for Liver and Digestive Health, Division of Medicine, University College London, Royal Free Campus, London, United Kingdom

HIGHLIGHTS

- A system model for liver function is used to study the effect of fructose on NAFLD.
- Model supports clinical evidence that high fructose causes hepatic lipid deposition.
- Synergistic effect of three interventions has been predicted to be the strongest.
- Systems models in combination with *in vivo* experiments help explore an organ system.

ARTICLE INFO

Article history:
Received 26 June 2022
Received in revised form 7 September 2022
Accepted 16 September 2022
Available online 23 September 2022

Keywords:
Liver model
Fructose Metabolism
Insulin Resistance
NAFLD
Computational Modelling
Systems Biology

ABSTRACT

Metabolic disturbances to the liver system can induce lipid deposition and subsequently cause non-alcoholic fatty liver disease (NAFLD). Increasing consumption of fructose has been proposed as a crucial risk component in the development of NAFLD.

Three potential therapeutic targets in the network were explored using a composite model of liver function. Introducing a fructose enriched diet under insulin resistance conditions was simulated to evaluate the effectiveness of the model in novel therapy design. *In vitro* experiments were conducted on rat liver samples to assess the robustness of the model predictions.

Synergistic application of all three interventional points *in silico* has been predicted as the most effective treatment to reduce lipid production under both moderate and severe insulin resistance conditions.

This study demonstrates how we can use system models together with *in vivo* experiments to explore the behaviour of the liver system in response to fructose variation and use it to help identify possible drug targets.

1. Introduction

The heartland of Process Systems Engineering research and practice has been in process manufacturing but in recent years the approach has been used to tackle other problem domains where there is chemical and physical change such as energy systems and environmental systems. The human body involves both chemical and physiological changes in many complex interactions. When considered in this light we can see that Chemical Engineers, and Process Systems Engineers in particular, can play a role in helping to make the most of the knowledge of physiology and metabolism that is becoming increasingly quantified, modelled and subject to computational (known as '*in silico*' in contrast to '*in vitro*' or experimental and '*in vivo*' in animals and humans) analysis.

Some Chemical Engineers have been working on modelling and experimental investigations in medical fields. For example, Yin (2007) considered challenges in virology and Netti et al. (1997) examined fluid transport in tumours. Peppas and Langer (2004)

Abbreviations: ADP, Adenosine Diphosphate; ATP, Adenosine Triphosphate; FA, Fatty Acid; FBP, Fructose-Bisphosphatase; GA3P, Glyceraldehyde-3-Phosphate; HFCS, High Fructose Corn Syrup; IR, Insulin Resistance; KHK, Fructokinase (also known as Ketohexokinase); NAFLD, Non-Alcoholic Fatty Liver Disease; NASH, Non-Alcoholic Steatohepatitis; PFK, Phosphofructokinase; PK, Pyruvate Kinase; PPARα, Peroxisome Proliferator-Activated Receptor Alpha; TG, Triglycerides.

* Corresponding author at: Centre for Process Systems Engineering, Department of Chemical Engineering, University College London, London, United Kingdom.
E-mail address: y.liao@ucl.ac.uk (Y. Liao).

https://doi.org/10.1016/j.ces.2022.118131
0009-2509/

reviewed the contributions of Chemical Engineers to Biomedical Engineering over the years concentrating on biomaterials, drug delivery and tissue engineering. Chemical Engineers have been engaged in looking at the Systems Engineering of medical systems (see Bogle (2012) and Vodovotz et al. (2013) for recent reviews and Parker and Clermont (2010) for an example of the inflammatory response to infection or trauma). The report 'Convergence: the Future of Health' (Sharp and Hockfield, 2017) sets out a range of challenges for bringing together disciplines, including Engineering, to solve healthcare problems highlighting imaging, nanotechnology, regenerative engineering and medicine, and big data.

The chemistry and biochemistry in these systems is hugely complex. The chemistry of life is a dynamic process governed by complex reaction networks, it is affected by personal genetics and is spatially distributed by being localised in specific organs and often in specialised cells. Reactions are of course not confined to the 'unit operations' (organs). There has been huge progress in unravelling the chemistry of life with vast databases of pathways, genetics, transcription factors and so on. It would eventually be necessary to be able to quantify fluid and transport properties (through cells, across membrane boundaries, and within fluid streams) where there has been considerable theoretical work but needs more modelling across scales and further data (Kapellos et al., 2010). This makes the need for a systems approach all the more necessary, not only to help link and solve the complexity but also to identify what crucial information is missing.

The 'design' and 'control' objectives for human operation are not simple. The control of the body, homeostasis, requires smooth and steady operation but this does not necessarily mean that key variables need to track a set point, although the system needs to keep these variables within bounds. Homeostasis ensures the following entities are 'kept, by carefully regulated mechanisms, within the narrow limits compatible with life': nutrients, O_2, CO_2, waste, pH, water, electrolytes, blood pressure and volume, and temperature (Sherwood, 2015). For example, glucose in the bloodstream needs to be kept within bounds to ensure neither hyperglycaemia or hypoglycaemia occurs. This is a key function of the liver system as amongst other functions, the liver and associated organs (such as muscle, kidneys, adrenal glands, the gastrointestinal tract and the hypothalamus) regulate the levels of glucose in the blood stream to ensure there is adequate energy available. Many of the functions are chemical and as such the liver can be seen as 'the chemical factory of the body'. In this paper we review research on modelling the liver system and report on some systems level model-based analysis of liver function, particularly in response to a fructose challenge which is a key source of energy alongside glucose, though lacking the same regulatory control points for its metabolism.

In Section 2 we review the state of modelling of the liver system particularly as it relates to an important disease, Non-Alcoholic Fatty Liver Disease (NAFLD), which is increasing in prevalence around the world due to its links with obesity. Section 3 presents the results using computational models exploring three specific scenarios of disease, NAFLD in particular, and compares to experimental (*in vitro*) results. Section 4 presents some conclusions and discusses how this model can be built into a wider set of system models to determine acceptable treatments taking account of wider system issues.

2. Exploring liver system behaviour

2.1. NAFLD and its causes

Despite the fact that the prevalence of NAFLD is increasing globally, its underlying pathophysiological mechanisms still remain poorly understood. Over the last decade, the proposed pathogenesis of NAFLD has evolved from the "two-hit" theory to the "multiple-hit" hypothesis (Buzzetti et al., 2016, Petta et al., 2016).

The "first hit" is simply intracellular lipid accumulation in the liver, often induced by sedentary lifestyle, obesity and metabolic syndrome leading to insulin resistance. Activating inflammatory factors causes the "second hit" leading to chronic hepatic inflammation. As well as lipid deposition and inflammation, the "multiple-hit" theory proposes that gastrointestinal microbiome imbalance, and hormonal dysregulation as well as other risk factors are also "hitting" the development of NAFLD and its progression to non-alcoholic steatohepatitis (NASH). These effectors occur in parallel and the first two hits do not necessarily appear in sequence (Buzzetti et al., 2016, Benedict and Zhang, 2017).

Hence, it is widely accepted that the pathogenesis of NAFLD is multifactorial and includes genetic, environmental, dietary and other metabolic factors including insulin resistance. Unsurprisingly, the ambiguity in the underlying mechanism of NAFLD directly results in the absence of effective therapeutic interventions. So far, lifestyle intervention is commonly recommended for NAFLD (and NASH) patients. Some medical treatments can be introduced to alleviate metabolic syndrome associated symptoms or to reduce obesity, which has an indirect impact on NAFLD-associated dysfunction, but to date no pharmaceutical drug has been approved specifically targeting NALFD as an identifiable disease.

Hepatic insulin resistance is recognized as a pathophysiological manifestation of NAFLD, metabolic syndrome often leading to type 2 diabetes. It occurs when cells such as hepatocytes lose their sensitivity to insulin meditated glucose uptake causing blood glucose levels to rise following meals (Santoleri and Titchenell, 2019). However, the causal relationship between hepatic insulin resistance and these diseases has not been definitively understood. For example, there is debate as to whether insulin levels can be stimulated by fructose consumption and whether a persistent high-fructose diet will lead to compensatory hyperinsulinemia, resulting in reduced sensitivity.

Increasingly, evidence suggests that NAFLD is a multisystem condition (Byrne and Targher, 2015) which is not only associated with liver-oriented diseases, but also contributes to chronic kidney disease (Byrne and Targher, 2020), cardiovascular disease (Anstee et al., 2013), hypertension (Ryoo et al., 2014), Type 2 Diabetes Mellitus (Fracanzani et al., 2008) and other chronic conditions. Typically, the lifestyle factors contributing to obesity have often been blamed as the cause of NAFLD though genetic predisposition is a key contributor. However, recent clinical and experimental studies repeatedly suggest that the trend of increasing consumption of fructose over recent decades may also be a crucial risk component, (e.g., Jensen et al. (2018)). It is speculated that high fructose intake would decrease tyrosine phosphorylation of the insulin receptor and damage insulin receptor substrate phosphorylation (Havel, 2005, Nomura and Yamanouchi, 2012), which suggests that fructose can cause insulin resistance by down regulating insulin mediated activity.

2.2. Existing computational models of liver systems

Recent dynamic liver models focus on the regulation of glucose homeostasis. Hetherington et al. (2012) applied an innovative engineering method to create a composite and flexible model to simulate hepatic glucose homeostasis regulated by glucagon and insulin based on liver-pancreas interaction. König et al. (2012) developed a hepatic kinetic model to represent glycolysis and gluconeogenesis pathways as well as glycogen metabolism. This model also examined the effect of hormonal regulation (insulin, glucagon and epinephrine) on glucose metabolism. On the basis

of glucose metabolism, Chalhoub et al. (2007) integrated part of the lipid metabolism (particularly fatty acids) into a dynamic computational model. Naftalin (2016) constructed a computer model to simulate glucose absorption and illustrated a relationship between this and metabolic diseases.

Much Chemical Engineering is based on lumped models as are some human organ models. If we are interested in glucose regulation in the bloodstream for diabetes for example, lumped models of liver and pancreas give good predictive utility and allow discovery of system behaviour characteristics (Ohno et al., 2008). As mentioned above, NAFLD is a condition in which accumulation of lipids and fat in the liver and liver cells (hepatocytes) arises from a malfunction of hepatocyte metabolism. Conditions such as NAFLD affect the liver cells across the liver sinusoid (the functional space between blood supply and venous removal of the blood flow) in a differential way resulting in the need for a distributed model. Most existing *in silico* modelling considers the liver as an ensemble piece but there are studies that have developed compartmental models to mimic the effects of 'zonation' (distributed behaviour) across the liver sinusoid to study the hepatic energy metabolism. An eight-compartment-model of simulating hepatic flexibility and elimination was introduced by Anissimov and Roberts (2002) using palmitate as the central parameter to make corresponding model predictions. The Ohno model (Ohno et al., 2008), which also has eight compartments, focuses on investigating the ammonia metabolism enabling the examination of the differing expression levels of three enzymes by including carbonyl phosphate synthase, glutamine synthase and ornithine aminotransferase within the compartments. The 8-compartment model of Ashworth et al. (2016) was used to explore the sensitivities of the model parameters resulting in the development of NAFLD and its precursor conditions considering only the glucose pathway.

Most previous models (lumped and distributed) have concentrated on glucose as the key nutrient to the system. Liao et al. (2020) developed a model of the fructose metabolism to explore behaviour particularly under high stress metabolic conditions which results in lipid accumulation as observed in diseases such as NAFLD.

2.3. Current model settings

The objective of this paper is to illustrate how a systems-based approach allows us to explore the effect of fructose, with glucose, in the development of NAFLD using an *in silico* model with some experimental verification. Liao et al. (2020) presented a detailed kinetic model of fructose metabolism and it is this model that has been utilised here. The published model involves 25 states, 25 ordinary differential equations, and 12 rate equations. The full model can be found in the supplementary material.

2.3.1. Insulin resistance simulation

Insulin resistance (IR) is one of the common pathophysiological features of NAFLD, even in non-obese patients, and subjects with IR are considered to be the high-risk population predisposed to NAFLD. The equations that involve the key parameters of IR which are explored in this study are given in Table 1. The model has the capability to explore system behaviour that might result from targeting one or more steps in the pathway (e.g., with drugs) that would supress or enhance specific reactions in the pathway.

Using the model, IR conditions were triggered by multiplying the insulin concentration by an IR parameter (see Table 1) with a value of less than one ($0 < IR < 1$), simulating cells in liver, muscle and adipose tissue that do not respond well to insulin. The values of IR = 0.5 and IR = 0.25 were assigned to represent moderate IR and severe IR conditions. The peak values of both hepatic and plasma concentrations of fatty acids and triglycerides were recorded for further analysis and validation.

2.3.2. The systemic and systematic search for interventional targets

Fig. 1 shows the pathways that cells utilise to take up nutrients (sugars) that enter the system from food we consume, specifically glucose and fructose. We have chosen to explore three specific potential therapeutic interventions, pyruvate kinase (PK), fructokinase (KHK) and peroxisome proliferator-activated receptors alpha (PPARα), because these are central components in the metabolic regulation for simple sugars as shown in Fig. 1.

The glucose and fructose pathways merge to produce glyceraldehyde 3 phosphate (GA3P). PK is the rate limiting enzyme to break down GA3P to pyruvate, releasing essential substrates for either energy production or lipid synthesis. Inhibiting PK is considered to be a potential intervention which can productively reduce fatty acid synthesis (Gassaway et al., 2019, Nain-Perez et al., 2022, Tiersma et al., 2022).

KHK is not limited by adenosine triphosphate (ATP) or citrate availability (as is the case of glucokinase in the glycolytic pathway) as part of the fructose phosphorylation process. Since this reaction is the first step in the fructose metabolism within the liver and it is exclusively contributing to the fructose metabolic pathway, suppressing this process can in principle, effectively prevent fructose-induced lipid accumulation.

Recent research has shed a new light on PPARα but its role in NAFLD still remains unclear. It has been proposed (Nomura and Yamanouchi, 2012) that the expression of PPARα might be inhibited by high production of fructose-1-phosphate, which leads to the decrease of beta-oxidation activity, causing fat accumulation in the liver. As a result, the capacity to clear lipid build-up in cells would be impaired, contributing to the development of NAFLD. Also, it has been reported by Murakami et al. (2022) and Padole et al. (2022) that applying a PPARα agonist can reduce liver fat in mice and in clinical patients. Therefore, PPARα activation is considered as a promising intervention to protect the liver from developing NAFLD after fructose over-consumption.

To demonstrate the power of the systems engineering approach to medical issues associated with fructose consumption, these three key metabolites in the network are explored here using a composite model of liver function with fructose as a substrate/nutrient.

2.3.3. Model simulations

Simulations were generated using MATLAB_R2019a (MATLAB, RRID:SCR_001622). The function 'ode45' was used to solve all the ordinary differential equations simultaneously. The default solver settings are listed in Table 2. The units of metabolite concentration and reaction rate are presented in micromoles/litre (μM/L) and micromoles/second (μM/s), respectively. The simulations have been set to run over a 12-hour period incorporating 3 meals. The nutrients for each of the 3 meals were introduced instantaneously. The initial values and parameter settings as well as MATLAB code are also provided in the supplementary material.

2.4. Confirming the experimental system

2.4.1. Animal samples and diet

Following the model predictions we report on some experimental work using fructose fed rats which, while not providing a complete verification which would be extremely difficult, aims to give confidence that the model predictions confirm animal behaviour. The materials and methods for these experiments are outlined here. In collaboration with Aarhus University, Denmark, 20 male Sprague Dawley rats were randomized into 2 groups. Over 16 weeks, rats received either a fructose enriched diet to model

Table 1
Fructose model equations which involve insulin resistance (IR) terms (adapted from Liao et al. (2020)).

Variables	Adipose Tissue, Muscle and rest of the Body
Blood Glucose	$\frac{dGlu_{SBC}}{dt} = Meal_{Glu} + C_{Glu} - USE_{Glu} - UP_{FA} * IR - UP_{TG}$
Fatty acids (Palmitate)	$\frac{dFA_{SBC}}{dt} = C_{FA} - USE_{FA} * IR + UP_{FA}$
Fatty acids (Palmitate) Cross-membrane Transportation	$T_{FA} = V_{FA}^{ex} * \frac{FA_{SHB} - FA_{SH}}{K_m^{FA-ex} + FA_{SHB} + FFA_{SH}} + V_{active} * \frac{FA_{SHB}}{(K_m^{active} + FA_{SHB})} \left(1 + \frac{Ins}{Ins_{ref}^{active}}\right) * IR$
Variables	**Hepatic Section**
Fructose-bisphosphatase (FBP)	$\mathbb{R}_{FBP} = V_{FBP} * \frac{GA3P}{K_m^{FBP} + GA3P} * IR$
Phosphofructokinase (PFK)	$\mathbb{R}_{PFK} = V_{PFK} * \frac{G6P}{K_m^{PFK} + G6P} * \frac{ATP}{Km_{ATPpfk} + ATP} * \left(1 - \frac{ATP}{ATP + k_i^{ATPpfk}} * \frac{ADP}{ADP + k_i^{ADPpfk}}\right) * \left(1 - \beta_{PFK} \frac{GA3P}{GA3P + k_i^{GA3Ppfk}}\right) * IR$
Pyruvate kinase	$\mathbb{R}_{PK} = V_{PK} * \frac{GA3P^{nGA3P}}{Km_{GA3P}^{nGA3P} + GA3P^{nGA3P}} * \frac{ADP^{nADPpk}}{Km_{ADPpk}^{nADP} + ADP^{nADPpk}} * \left(1 - \beta_{ACoA-PK} \frac{ACoA}{K_i^{ACoA-PK} + ACoA}\right) * IR$
Phosphoenolpyruvate carboxykinase	$\mathbb{R}_{PEPCK} = V_{PEPCK} * \frac{Pyr}{K_m^{PEPCK} + Pyr} * \frac{ATP}{K_m^{ATPpepck} + ATP} * \frac{GTP}{K_m^{GTP} + GTP} * IR$
Pyruvate oxidation	$\mathbb{R}_{PDC} = V_{PDC} * \frac{Pyr}{K_m^{Pyr} + Pyr} * \left(1 - \beta_{ACoA-PDC} \frac{ACoA}{ACoA + k_i^{CoA-pyr}}\right) * IR$
Fatty acid synthesis	$\mathbb{R}_{FAS} = V_{FAS} * \frac{ACoA}{K_m^{ACoA} + ACoA} * \frac{ATP}{K_m^{ATPfas} + ATP} * \left(1 - \beta_{FA} \frac{FA}{FA + k_i^{FA-inhib}}\right) * IR$
Beta-oxidation	$\mathbb{R}_{boxi} = V_{boxi} * \frac{FA}{K_m^{boxi} + FA} * \frac{ATP}{K_m^{ATPboxi} + ATP} * \left(1 - \beta_{boxi} \frac{ACoA}{ACoA + k_i^{CoA-boxi}}\right) * \left(1 - \beta_{PPAR\alpha} \frac{F1P}{F1P + k_i^{F1P-inhib}}\right) * IR$
Triglyceride synthesis	$\mathbb{R}_{TGS} = V_{TGS} * \frac{FA}{K_m^{FA} + FA} * \frac{GA3P}{K_m^{GADP} + GADP} * IR$
Lipolysis	$\mathbb{R}_{Lply} = V_{Lply} * \frac{TG}{K_m^{TG} + TG} * IR$

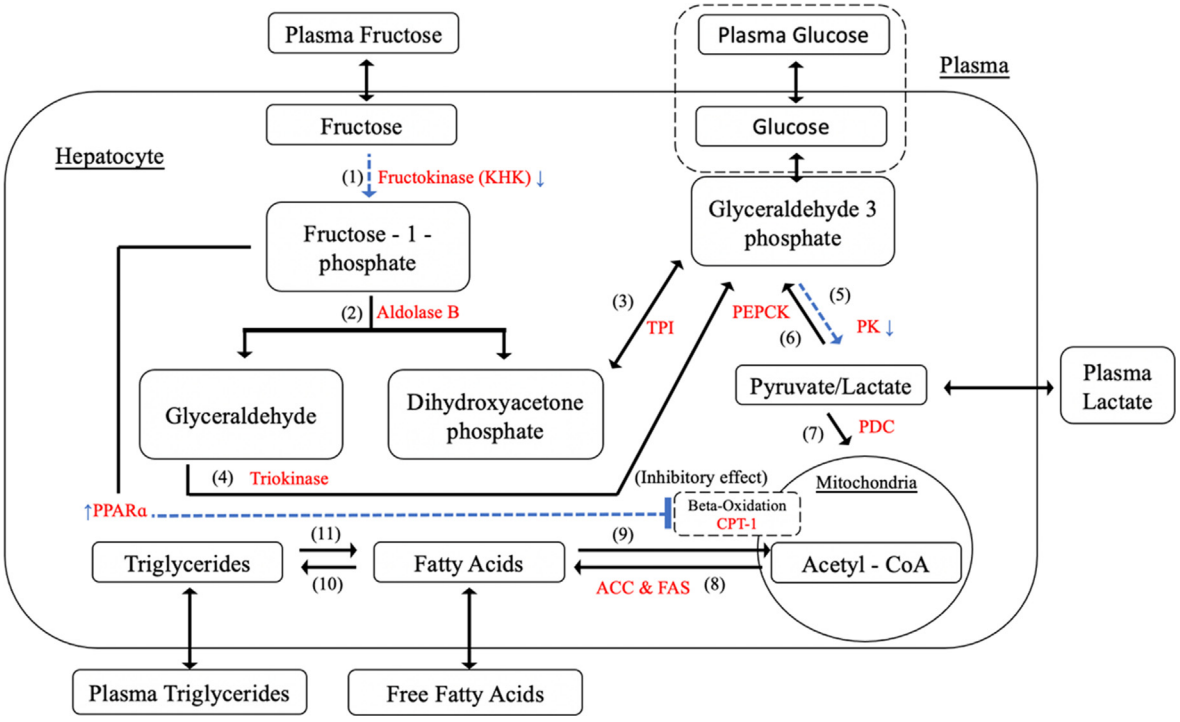

Fig. 1. Hepatic fructose metabolism with interventional treatments. (The blue dashed lines indicate where reaction is reduced). (For interpretation of the references to colour in this figure legend, the reader is referred to the web version of this article.)

Table 2
Function 'ode45' solver setting.

Function	Stage	Order	Solver type	Method
ode45	Six	Fifth	Single-step; Solve non-stiff differential equation	An explicit Runge-Kutta (4,5) formula (the Dormand-Prince pair)

NAFLD or normal rat chow. One rat in the fructose group was found dead at week 15 as an unrelated event; hence, frozen liver tissues from 10 rats in the control group and 9 rats in the fructose group were analysed for the biochemical experiments.

The caloric intake distribution provided by the control diet and fructose diet per 100 g chow are shown in Fig. 2. In the control diet 12.35 % of calories were supplied by fat, which means the percentage is approximately 3 % higher than that in the fructose diet. How-

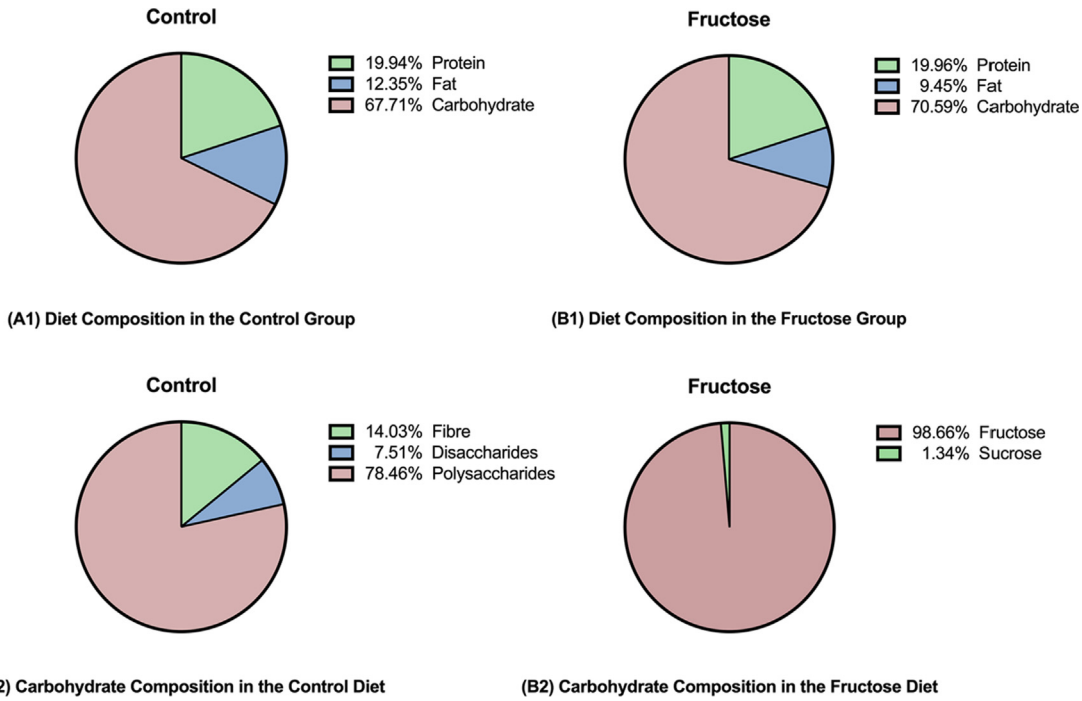

Fig. 2. Diet compositions regarding energy contribution in the animal experiments. (A1 and B1: the compositions of diet in the control group and the fructose group; A2 and B2: the composition of carbohydrates in the control diet and the fructose diet.).

ever, this 3 % energy discrepancy is compensated by the source of carbohydrate in the fructose group.

At Week 16, the subjects were terminated and dissected. Portal blood, arterial blood and tissues were collected for further research purposes. In the current study, only the liver pieces were used for the examinations.

2.4.2. BCA protein assay

The BCA protein assays are one of the most commonly used measurements for total protein quantification. Assays were conducted according to manufacturer's instructions (Thermo Fisher, 23225). The methodology in detail is provided in the supplementary material.

2.4.3. Western blotting

Western blotting was used to measure the protein expression levels of KHK and PPARα. The aim of this assay is to quantify the amount of KHK and PPARα in order to test whether fructose feeding would upregulate or downregulate the expression of these two key targets in the fructose metabolic pathways. Tissue extracts were prepared by homogenizing samples of liver. The detailed protocol of western blotting is provided in the supplementary material.

2.4.4. Enzymatic activity assay

The enzymatic activity assays of pyruvate kinase (PK), fructokinase (KHK) were performed adapting Worthington's method (Worthington, 1988) and Groisillier and Tonon's approach (Groisillier and Tonon, 2015), respectively, to explore whether the reaction rates of these two crucial enzymes would be affected by high fructose consumption. The detailed steps and calculations are provided in the supplementary material.

2.4.5. Image analysis and data statistical analysis

At least triplicate data were collected to calculate means and standard deviations (SD) for all the results in this project. Data from the 96 well plate reader was analysed through the OMEGA-MARS Data Analysis System, Microsoft Excel software and GraphPad Prism 7 software. T-test analysis was performed to compare the disparities between the control group and the experimental group. A P-value<0.05 was accepted as a statistically significant difference.

3. Results and discussion

3.1. Model performance under insulin resistance conditions

Before constructing any scenarios, model performance evaluations under both normal and abnormal metabolic conditions were undertaken and are presented in Fig. 3. A 50/50 fructose/glucose diet (representative of normal table sugar) was set as the standard

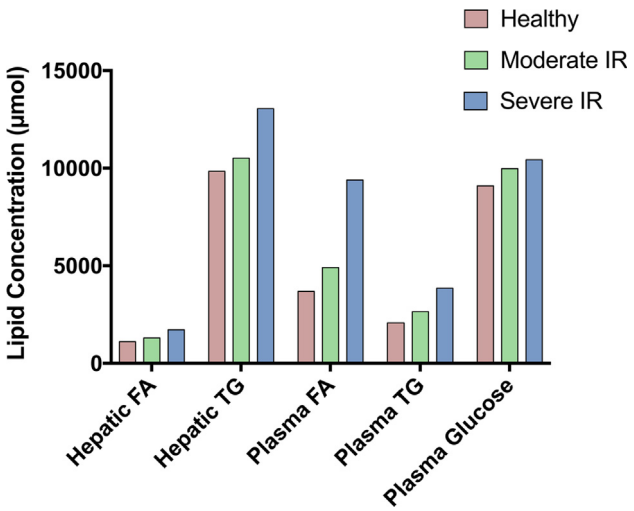

Fig. 3. Lipid deposition after moderate IR and severe IR simulation.

input and the simulations were run for twelve hours for acute effect consideration.

It can be observed that higher concentrations of lipids were produced under IR environments, compared to normal healthy conditions. Blood glucose level was also higher under IR conditions, consistent with the mechanism that impaired insulin sensitivity often fails to regulate blood glucose homeostasis. Meanwhile, when the more extreme IR condition parameters were used, a more severe lipid deposition was found to develop, especially reflected in hepatic triglycerides (TG) and plasma fatty acids (FA). These phenomena imply that severe insulin resistance has the result of inducing simple lipid accumulation, acting as a precursor to the early stages of NAFLD.

To further test model performance under impaired insulin sensitivity situations, two scenarios were created. Different kinds of compositions for dietary design were simulated accordingly, mimicking isocaloric carbohydrate intake and hypercaloric fructose intake.

3.1.1. Scenario one: Isocaloric carbohydrate intake with impaired insulin sensitivity

In this scenario, the isocaloric meals comprising different combinations of monosaccharides (50:50 or 60:40 for fructose:glucose) were introduced as the dietary inputs. These two specific diets represent sucrose and high fructose corn syrup (HFCS), respectively. The reason for these input choices is that they represent the commonest forms of fructose consumption. The simplification was made that sucrose breaks down into fructose and glucose directly in 1:1 ratio following absorbance in the body. Therefore, the data in Fig. 3 is used as sucrose consumption in Fig. 4. A total of 100 g of carbohydrates were introduced in each cycle. The changes in lipid profiles as well as in blood glucose level are summarised in Fig. 4.

Under the healthy status, the HFCS feeding group produced higher concentrations of both hepatic and plasma FA than the sucrose feeding group. For TG profiles little variation was seen between the sucrose consuming group and the HFCS feeding group. These predictions are in accordance with the findings reported by Stanhope et al. (2008) and Stanhope et al. (2009), suggesting that HFCS is likely to enhance hepatic *de novo* lipogenesis as it contains 10 % more fructose than sucrose.

When insulin sensitivity is impaired a similar pattern was observed in FA profiles, which is consistent with the outcomes presented by Abraha et al. (1998). In terms of the TG levels, it can be seen that HFCS, in comparison to sucrose, contributes to a higher hepatic TG production but a lower plasma TG secretion under the moderate IR condition. This suggests that consuming high fructose content feed tends to cause hepatic lipid deposition but not systemic fat accumulation.

It is worth mentioning that some surprising results were identified when the IR condition became more extreme. Theoretically, the HFCS group is expected to generate a higher triglyceride level than the sucrose group as HFCS has a higher proportion of fructose. However, as shown in Fig. 4(B) and (D), the model predictions show that less hepatic TG was generated in the HFCS group compared to the sucrose group and the difference between the two groups was observed in the plasma TG level. This unexpected behaviour can be explained by the insulin regulation setup in the model. During model development, insulin resistance is considered to have a larger effect on glucose metabolism while fructose is effectively insulin-independent. Due to the progressive reduction in sensitivity, even if more insulin is produced, the net effect is that cells take up less glucose. The model reflects the impact of decreased glucose uptake in an IR individual and, in this case, insulin is not attributed any other functions – though in the body it does elicit other effects. Therefore, when a large amount of insulin is released under severe IR conditions, the glucose components are affected to a greater extent relative to fructose, causing higher TG production in the sucrose group.

In relation to blood glucose, sucrose consumption induces a higher level than HFCS for both healthy and unhealthy status parameters. The results are as expected since insulin secretion is considered not to be triggered by fructose intake and sucrose has proportionately more glucose in comparison to HFCS.

To sum up, the effect of isocaloric carbohydrate intake combined with impaired insulin sensitivity on lipid production was assessed in the current scenarios. The results indicate that the model is capable of making rational predictions under abnormal metabolic conditions. However, the performance under severe IR simulation is limited.

3.1.2. Scenario Two: Hypercaloric fructose intake with impaired insulin sensitivity

In order to test model versatility, a hypercaloric fructose intake scenario combined with impaired insulin sensitivity was created to represent a worst-case scenario. In reality, it is against the no-harm policies and experimental ethics to replace all the carbohydrate source with fructose for a clinical experimental design. However, computational modelling has the advantage of being able to simulate an unrealistic, excessive amount of fructose exposure without any ethical concerns.

Considering fructose is naturally consumed with glucose, the hypercaloric fructose diets were set with an addition of 50 g glucose per meal. The three simulated diets are: a baseline diet (50 g fructose per meal), a high fructose diet (a 12.5 % increase in fructose) and a very high fructose diet (a 25 % increase in fructose). Both moderate and severe IR environments were simulated.

The effects of hypercaloric fructose consumption on lipid accumulation combined with IR conditions are presented in Fig. 5. As shown in the figure, concentrations of all four kinds of lipids increase in a dose-dependent manner. Furthermore, as the IR condition that the model simulates worsens more substantial fat deposition was observed.

It should be noted that the high fructose diet was selected to represent a simple pro-steatosis condition (the early phrase in NAFLD development), in which 7.5 % and 26.1 % increases in hepatic triglycerides were observed under moderate and severe IR status, respectively. This setting fitted into the criterion of mild steatosis (Petäjä and Yki-Järvinen, 2016). Hence this high fructose diet (62.5 g fructose + 50 g glucose/meal) combined with IR conditions was applied to induce pro-steatosis conditions for potential treatment exploration in the following section.

Overall, two scenarios have been applied at this stage to examine whether the constructed model has the capability to make solid predictions under pathological conditions. In the next section, the proposals for synergistic drug treatments are explored.

3.2. Model based NAFLD analysis and synergistic treatment exploration

The current section focuses on the effects of potential interventional targets on early stage of NAFLD, which appears as simple lipid deposition.

As stated above in section 3.1.2, a total of 62.5 g fructose with an addition of 50 g glucose was employed for each meal as dietary input, representing a high fructose feeding scenario. In addition, two abnormal conditions including moderate and severe IR were simulated to represent the two degrees of pro-steatosis conditions. Three practical interventions are introduced: −50 % suppression of PK, −50 % inhibition of KHK and +50 % activation of PPARα.

The synergistic effects of these interventions have also been assessed. The pairwise comparisons were conducted in order between the three potential targets. These simulations explore

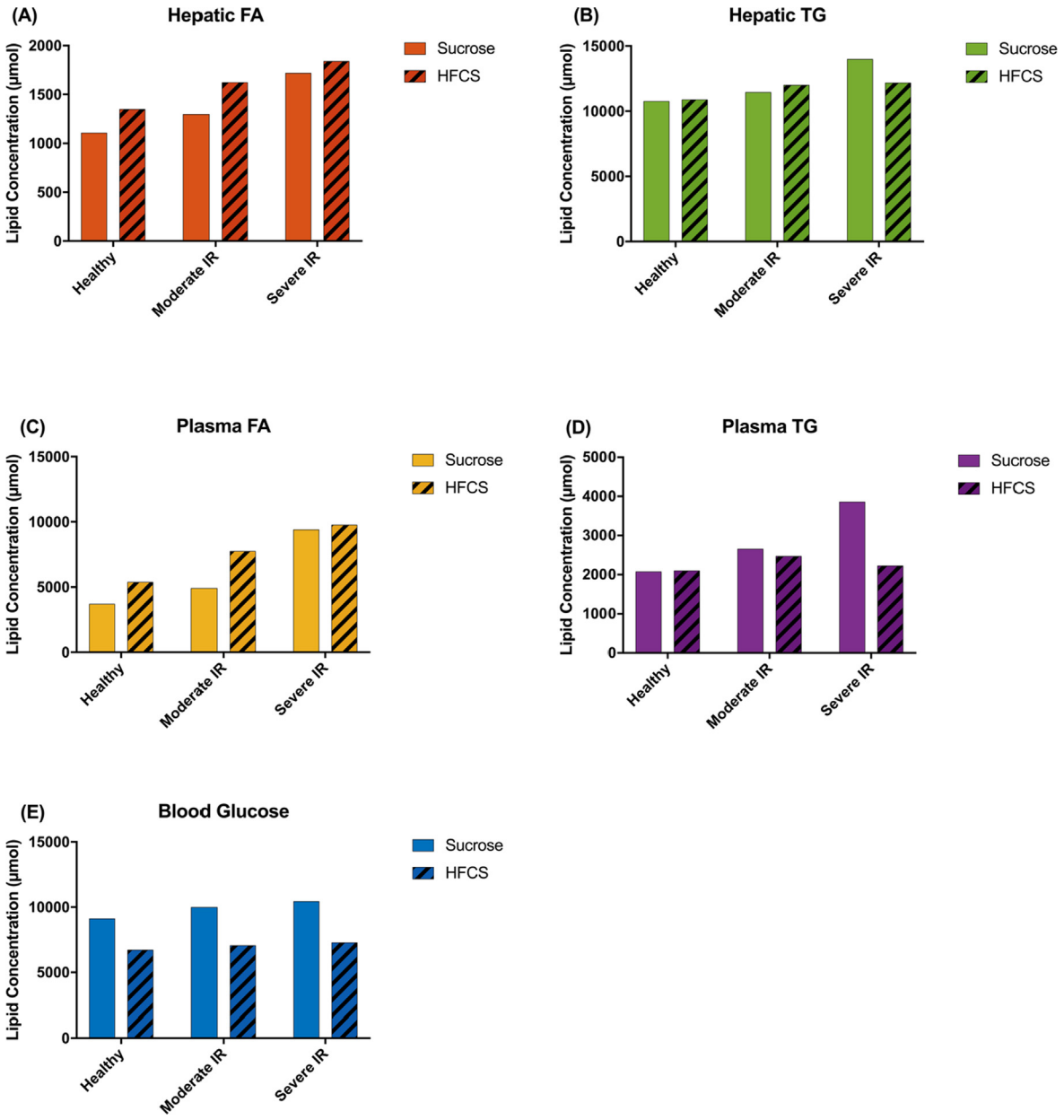

Fig. 4. The changes of lipid profiles after different dietary intakes combined with IR. (A) Hepatic FA, (B) Hepatic TG, (C) Plasma FFA, (D) Plasma TG, and (E) Blood Glucose. * The data shown above in Fig. 3 is included here as Sucrose for comparison with HFCS.

the effectiveness and robustness of the current model in novel therapy design.

The results of the pairwise comparisons between three interventions are shown in Fig. 6 and Fig. 7, presenting hepatic fatty acids and hepatic triglycerides, respectively. It should be noted that the plots of PPARα activation and PPARα + PK overlap completely in panel (F) of these two figures.

In Fig. 6, it can be seen from panel (A) that inhibiting PK by 50 % is able to reverse the hepatic fatty acid build-up condition back to a healthy level when insulin sensitivity is mildly impaired. Compared to PK, KHK suppression exerted a similar effect on preventing fatty acid synthesis. Lower levels were observed as a result of dual inhibition of PK and KHK. As insulin resistance progressed to a more severe condition in Fig. 6(B), suppressing KHK appears to be more effective than inhibiting PK for decreasing fatty acid concentrations. However, when applying the PK and KHK interventions simultaneously, the fatty acid levels were not observed to return to normal.

In addition, as shown in panel (C) to (E), the outcome of increasing PPARα expression by 50 % on controlling fatty acid level is extremely positive, regardless of the severity degree of insulin resistance. Enhancing PPARα expression enables a decrease in hepatic fatty acid accumulation significantly. Under moderate IR condition, the synergistic effect of PPARα and PK is as effective as the combination of three treatments, suggesting that KHK is the least efficient interventional target among the three tested by the model. When severe IR was simulated, the situation is slightly different as the least impact was observed after suppressing PK activity.

In terms of hepatic triglyceride levels, a similar reverse pattern can be perceived under the moderate IR condition, as shown in Fig. 7(A), (C) and (E). However, the results are rather interesting when insulin resistance is increased. It can be observed from Fig. 7(B) that inhibiting PK boosts triglyceride production in the liver, instead of decreasing it as expected. The triglyceride level after PK treatment is even higher than that under the pro-steatosis condition.

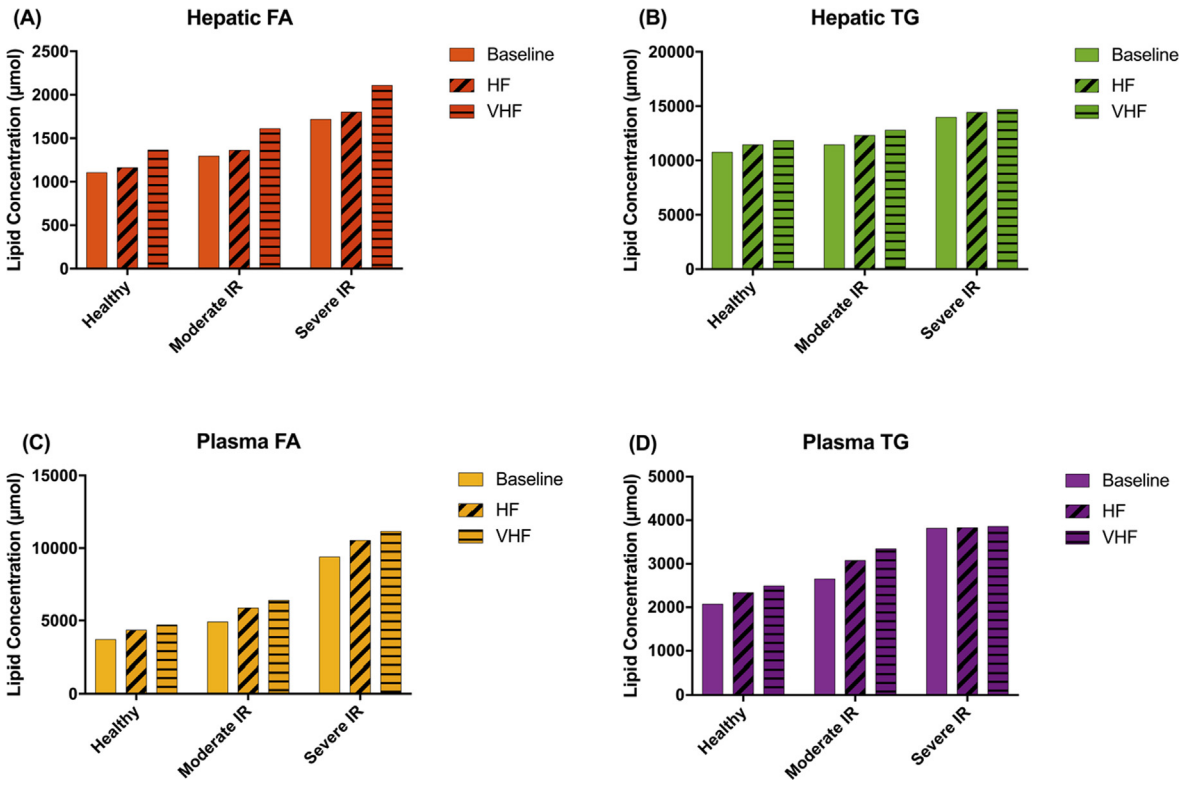

Fig. 5. The change of lipid accumulation after different fructose intakes combined with IR. HF: A high fructose diet; VHF: a very high fructose diet. (A) Hepatic FA, (B) Hepatic TG, (C) Plasma FFA, and (D) Plasma TG.

At the model construction level, the reason why PK suppression surprisingly leads to triglyceride accumulation can be elucidated by Fig. 1 and the triglyceride synthesis process (which consumes three fatty acid molecules and one glycerol backbone from glycerol-3-phosphate to produce triglyceride). As highlighted in Fig. 1, when PK is inhibited, the amount of GA3P would increase and subsequent metabolites after pyruvate are expected to decrease. However, excess GA3P is then used to synthesize triglyceride, causing triglyceride over-production.

Overall, based on the model predictions, all three interventional approaches have the capability to reduce fatty acid deposition under moderate IR conditions. PPARα activation is the most stable treatment that would not be affected by the degree of insulin sensitivity impaired and plays a dominant role in the combination treatment studies.

3.3. Experimental assessment and validation

As mentioned in section 2.3.2, PK, KHK and PPARα are the three interesting interventional targets. Given that the model is built at a protein expression level, these proteins were made the priority in the experimental work. Therefore, two experimental tests, western blotting and enzymatic activity assays, were carried out to evaluate whether the expression levels and activity rates of these potential intervention points were altered by different carbohydrate diets.

3.3.1. The effect of different carbohydrates on KHK and PPARα expressions

To evaluate whether a high fructose diet alters protein expression of KHK and PPARα, western blotting analysis of liver tissue from the rat model was performed. Since KHK and PPARα are considered to be the more fructose-specific components, only these proteins were assessed.

Two questions are answered here: 1) whether fructose has the capability to trigger more KHK expression, converting fructose to fructose-1-phosphate and delivering abundant substrates for subsequent lipogenesis reactions; and 2) whether fructose has an inhibitory effect on PPARα that results in less β-oxidation and more lipid deposition.

The conservatively expressed protein β-Tubulin was used as the loading control to normalise the expression value and account for any preparation differences. The protein expression level is detected by a chemiluminescent method and quantified by its optical density. The results are presented in Fig. 8.

Although no statistical difference was found between the control group and the fructose group in both KHK and PPARα expression, it can be seen that KHK was up-regulated in the livers of rats fed with the high-fructose diet while hepatic PPARα was down-regulated. These results are in accordance with other studies in terms of KHK (Della Casa et al., 2016, Ishimoto et al., 2012, Roncal-Jimenez et al., 2011) and in PPARα (Schultz et al., 2015, Schmilovitz-Weiss et al., 2013, Roglans et al., 2007), suggesting that high-fructose consumption elevates KHK expression and suppresses PPARα expression.

Since the result from western blot experiment shows the increasing KHK expression after fructose-enriched meals, when combined with the model predictions in Fig. 6 (C, D) and Fig. 7 (C, D) in which inhibited KHK reduced hepatic lipid profiles back to normal levels in moderate IR and relatively lower in severe IR cases, it can be speculated that KHK inhibition is a promising way to reverse pro-steatosis conditions. Similarly, as shown in Fig. 8(B) and in Fig. 6(C, D) and Fig. 7(C, D) PPARα expression was suppressed by high-fructose consumption and the model predicts that activating PPARα could greatly alleviate lipid accumulation in the liver under both moderate and severe IR conditions. This suggests that PPARα is a promising target and inducing PPARα expression would be an effective treatment for

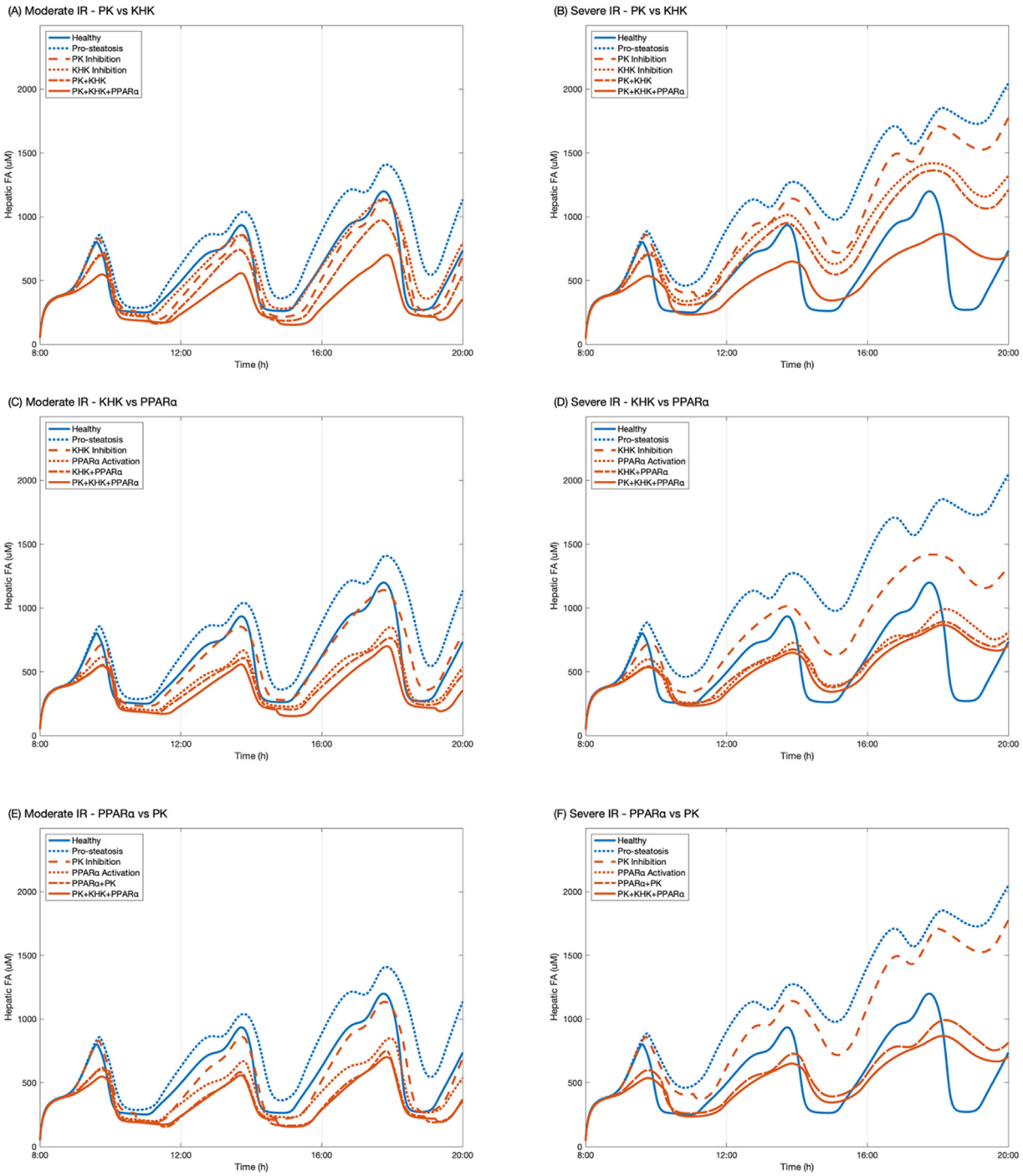

Fig. 6. The effects of three potential therapeutic targets on hepatic fatty acids. Pairwise comparisons: (A) (B) PK vs KHK, (C) (D) KHK vs PPARα, (E) (F) PPARα vs PK. (Three meals were simulated at time points 8:00, 12:00 and 16:00, respectively).

early-stage non-alcoholic fatty liver disease. The predictions could be further validated by conducting an experiment to test the synergistic effect of decreasing KHK and activating PPARα expressions synergistically.

3.3.2. The effect of High-Fructose diet on enzymatic activities of PK and KHK

The activity rates of the two enzymes PK and KHK were examined through enzymatic activity assays. PPARα was not assessed in this manner because it is a transcription factor rather than an enzyme which means it is unable to catalyse chemical reactions. The assay identifies whether there are any effects on changing reaction rates of PK and KHK metabolically after consuming a fructose-enriched diet.

A total of 60 cycles of absorbance values were recorded over 30 min. The decrease in optical density at 340 nm was measured quantitatively to reflect the reaction rate. Only the values during the time period of 6–8 min for PK and 2–4 min for KHK were analysed, as the values within these periods are considered to be the maximum rates of reactions, which is shown in Fig. 9(A1) (B1), before the reactions slowed due to a lack of substrate availability. The results are presented in Fig. 9.

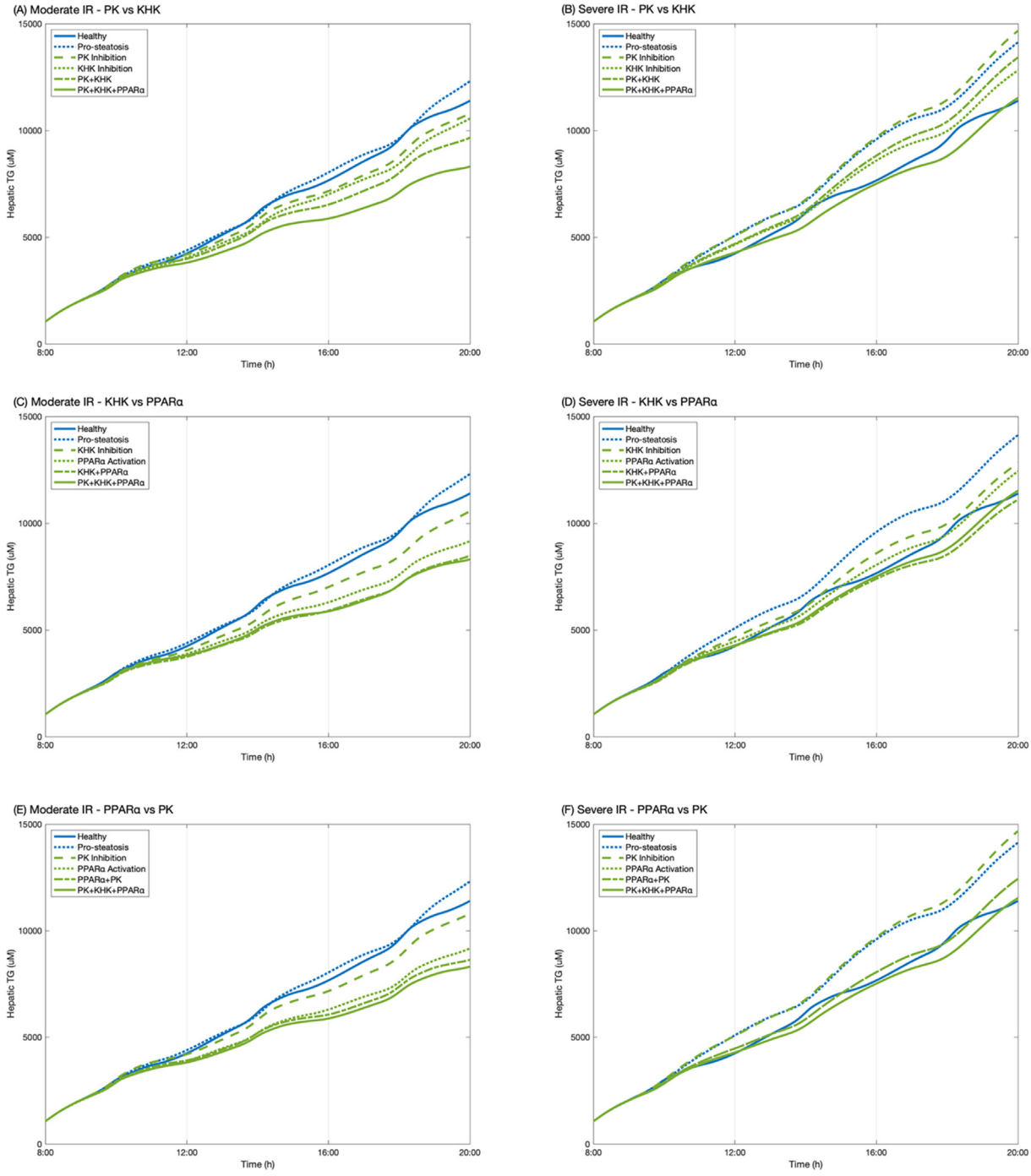

Fig. 7. The effects of three potential therapeutic targets on hepatic triglycerides. Pairwise comparisons: (A) (B) PK vs KHK, (C) (D) KHK vs PPARα, (E) (F) PPARα vs PK. (Three meals were simulated at time points 8:00, 12:00 and 16:00, respectively).

For PK activity, the slopes of the lines for each group as shown in Fig. 9(A1) indicate that values in the control group are higher than those in the fructose group run in parallel. The calculated averages for the PK reaction rates presented in Fig. 9(A2) are 3.08 ± 1.15 IU and 1.93 ± 0.41 IU for normal and fructose-fed rats, respectively.

However, the KHK slope of the fructose group has a steeper gradient than that of the control indicating that the reaction rate of KHK is faster in the fructose group. It can also be observed in Fig. 9(B2) that the KHK activity rate is significantly higher ($P = 0.0297$) in the rats exposed to the high-fructose diet than those fed with the normal chow i.e., 4.1 ± 0.56 IU for the former and 1. 84 ± 0.39 IU for the latter.

These results show that high-fructose consumption caused a reduction in PK activity. However, no significant difference was found between these two groups most likely due to a small sample size. For KHK, a fructose enriched diet increased the reaction rate and a statistical significance between groups was observed ($p < 0.05$). Combining with the results from western blotting in Fig. 8(A), it can be concluded that high fructose feeding can induce hepatic fat accumulation through regulating protein expression levels (e.g., PPARα), and/or increasing enzymatic reaction rates (e.g., KHK).

These experimental results coincide with the predictions in Fig. 6(A, B) and Fig. 7 (A, B), where limiting PK reaction rate is not as effective as inhibiting KHK reaction rate, especially when

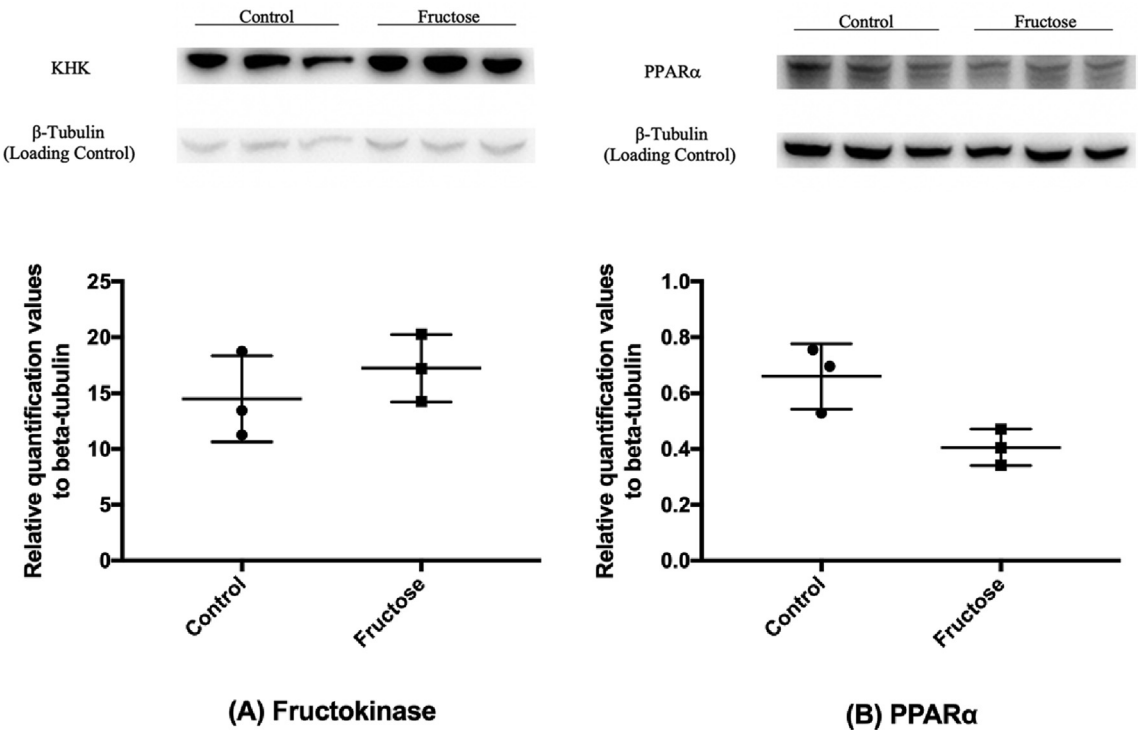

Fig. 8. The effect of different diets on KHK and PPARα expression. (The upper figure shows the KHK and PPARα bands. The amount of protein loaded was confirmed by the loading control in each lane; The bottom scatter plots shows the relative protein levels of KHK and PPARα in the liver samples. Control: n = 3; Fructose: n = 3).

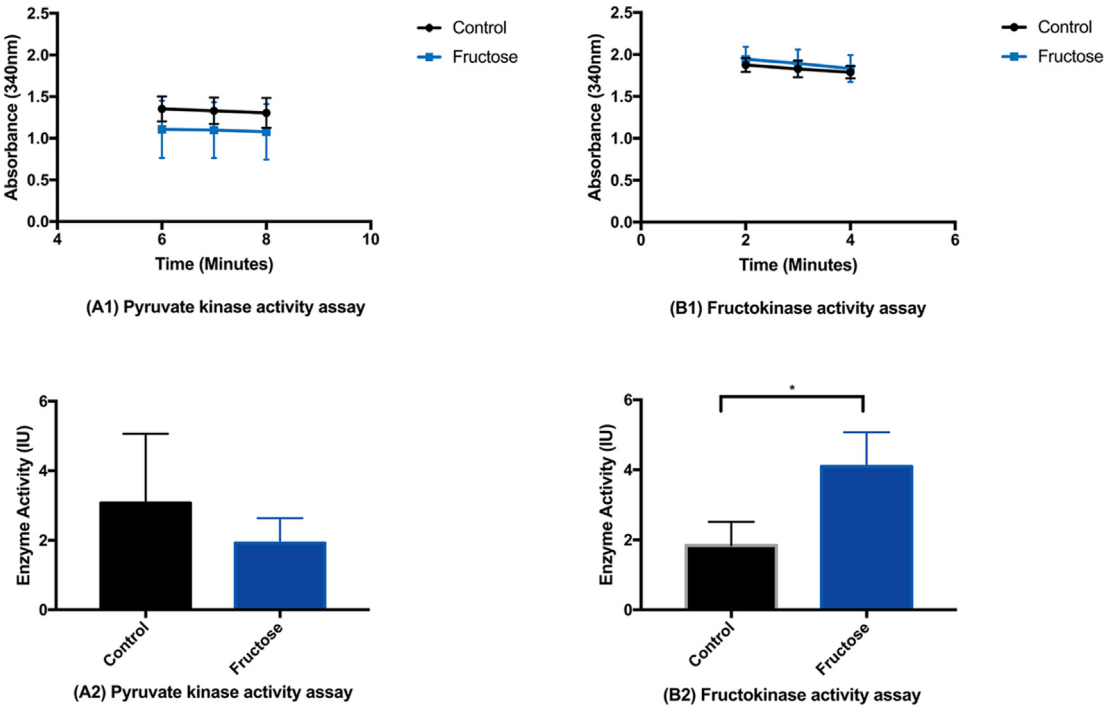

Fig. 9. The effect of different diets on PK and KHK activities. (A1 and B1 shows the optical density values in means ± SD of PK and KHK within the time periods; A2 and B2 are the scatter plots with single value and means ± SD, representing the average reaction rates of PK and KHK after calculation. Control: n = 3; Fructose: n = 3). $^{*}p < 0.05$, $^{**}p < 0.01$, $^{***}p < 0.001$ vs Control. IU: μmol/min/litre.

the IR condition is severe, and suppressing PK has minimal impact on lipid levels in the liver. While not validating all aspects of the model it does give confidence in the validity of the predictions.

Synergistic interventions to all three therapeutic targets (PK, KHK and PPARα) should be assessed experimentally to further validate the robustness of the constructed fructose model and its predictions. Through applying KHK inhibitor, PK inhibitor, PPARα agonist, and a combination of these three to an animal model, the results of lipid quantification assay then can be used to compare with the model predictions on the same graph.

4. Conclusions

The simulations above suggest that a high-fructose intake combined with insulin resistance would greatly accelerate hepatic lipid accumulation. The model has the capability to reproduce the kinetic relationship between fructose and lipid in the liver under insulin-resistant conditions. A synergistic intervention of PK, KHK and PPAR has been tested computationally as the most effective treatment to reduce the production of both fatty acids and triglycerides under both moderate and severe IR conditions. However, it should be noted that PPARα is considered as the most suitable therapeutic target because of its dominant and consistent behaviour during the simulation. In addition, stimulation of KHK as well as suppression of PPARα expression was observed in the high fructose feeding in the rat model. The experimental results support the model predictions for interventional targets.

This study demonstrates how we can use systems models together with *in vivo* experiments to explore the behaviour of the liver system in response to fructose variation and use it to help identify possible drug targets to prevent or reduce the effects of disease. The approach could be used on other systems where disease is the result of metabolic effects.

CRediT authorship contribution statement

Yunjie Liao: Conceptualization, Methodology, Software, Formal analysis, Writing – original draft. **Nathan A. Davies:** Writing – review & editing, Supervision. **I. David L. Bogle:** Writing – review & editing, Supervision.

Data availability

I have shared the link to my code at the Attach File step

Declaration of Competing Interest

The authors declare that they have no known competing financial interests or personal relationships that could have appeared to influence the work reported in this paper.

Acknowledgments

Thanks Dr Karen Louise Thomsen from Aarhus University for generously sharing the rat liver samples.

Funding

YL has been supported by UCL-CSC Joint Research Scholarship.

Appendix A. Supplementary material

Supplementary data to this article can be found online at https://doi.org/10.1016/j.ces.2022.118131.

References

Abraha, A., Humphreys, S.M., Clark, M.L., Matthews, D.R., Frayn, K.N., 1998. Acute effect of fructose on postprandial lipaemia in diabetic and non-diabetic subjects. Br. J. Nutr. 80, 169–175.
Anissimov, Y.G., Roberts, M.S., 2002. A compartmental model of hepatic disposition kinetics: 1. Model development and application to linear kinetics. J. Pharmacokinet Pharmacodyn. 29, 131–156.
Anstee, Q.M., Targher, G., Day, C.P., 2013. Progression of NAFLD to diabetes mellitus, cardiovascular disease or cirrhosis. Nat. Rev. Gastroenterol. Hepatol. 10, 330.
Ashworth, W.B., Davies, N.A., Bogle, I.D.L., 2016. A computational model of hepatic energy metabolism: understanding zonated damage and steatosis in NAFLD. PLoS Comput. Biol. 12, e1005105.
Benedict, M., Zhang, X., 2017. Non-alcoholic fatty liver disease: an expanded review. World J. Hepatol. 9, 715.
Bogle, I., 2012. Recent developments in Process Systems Engineering as applied to medicine. Curr. Opin. Chem. Eng. 1, 453–458.
Buzzetti, E., Pinzani, M., Tsochatzis, E.A., 2016. The multiple-hit pathogenesis of non-alcoholic fatty liver disease (NAFLD). Metabolism 65, 1038–1048.
Byrne, C.D., Targher, G., 2015. NAFLD: a multisystem disease. J. Hepatol. 62, S47–S64.
Byrne, C.D., Targher, G., 2020. NAFLD as a driver of chronic kidney disease. J. Hepatol. 72, 785–801.
Chalhoub, E., Hanson, R.W., Belovich, J.M., 2007. A computer model of gluconeogenesis and lipid metabolism in the perfused liver. Am. J. Physiol.-Endocrinol. Metab. 293, E1676–E1686.
Della Casa, L., Rossi, E., Romanelli, C., Gibellini, L., Iannone, A., 2016. Effect of diets supplemented with different conjugated linoleic acid (CLA) isomers on protein expression in C57/BL6 mice. Genes Nutr. 11, 26.
Fracanzani, A.L., Valenti, L., Bugianesi, E., Andreoletti, M., Colli, A., Vanni, E., Bertelli, C., Fatta, E., Bignamini, D., Marchesini, G., Fargion, S., 2008. Risk of severe liver disease in nonalcoholic fatty liver disease with normal aminotransferase levels: a role for insulin resistance and diabetes. Hepatology 48 (3), 792–798.
Gassaway, B.M., Cardone, R.L., Padyana, A.K., Petersen, M.C., Judd, E.T., Hayes, S., Tong, S., Barber, K.W., Apostolidi, M., Abulizi, A., 2019. Distinct hepatic PKA and CDK signaling pathways control activity-independent pyruvate kinase phosphorylation and hepatic glucose production. Cell Rep. 29 (3394–3404), e9.
Groisillier, A., Tonon, T., 2015. Determination of Fructokinase Activity from Zobellia galactanivorans. BIO-Protocol 5 (21).
Havel, P.J., 2005. Dietary fructose: implications for dysregulation of energy homeostasis and lipid/carbohydrate metabolism. Nutr. Rev. 63, 133–157.
Hetherington, J., Sumner, T., Seymour, R., Li, L., Rey, M.V., Yamaji, S., Saffrey, P., Margoninski, O., Bogle, I., Finkelstein, A., 2012. A composite computational model of liver glucose homeostasis. I. Building the composite model. J. R. Soc. Interface 9, 689–700.
Ishimoto, T., Lanaspa, M.A., Le, M.T., Garcia, G.E., Diggle, C.P., Maclean, P.S., Jackman, M.R., Asipu, A., Roncal-Jimenez, C.A., Kosugi, T., 2012. Opposing effects of fructokinase C and A isoforms on fructose-induced metabolic syndrome in mice. In: Proceedings of the National Academy of Sciences, p. 201119908.
Jensen, T., Abdelmalek, M.F., Sullivan, S., Nadeau, K.J., Green, M., Roncal, C., Nakagawa, T., Kuwabara, M., Sato, Y., Kang, D.-H., 2018. Fructose and sugar: a major mediator of non-alcoholic fatty liver disease. J. Hepatol. 68, 1063–1075.
Kapellos, G.E., Alexiou, T.S., Payatakes, A.C., 2010. Theoretical modeling of fluid flow in cellular biological media: an overview. Math. Biosci. 225, 83–93.
König, M., Bulik, S., Holzhütter, H.-G., 2012. Quantifying the contribution of the liver to glucose homeostasis: a detailed kinetic model of human hepatic glucose metabolism. PLoS Comput. Biol. 8, e1002577.
Liao, Y., Davies, N.A., Bogle, I.D.L., 2020. Computational Modeling of Fructose Metabolism and Development in NAFLD. Front. Bioeng. Biotechnol., 8
Murakami, K., Sasaki, Y., Asahiyama, M., Yano, W., Takizawa, T., Kamiya, W., Matsumura, Y., Anai, M., Osawa, T., Fruchart, J.-C., Fruchart-Najib, J., Aburatani, H., Sakai, J., Kodama, T., Tanaka, T., 2022. Selective PPARα modulator pemafibrate and sodium-glucose cotransporter 2 inhibitor tofogliflozin combination treatment improved histopathology in experimental mice model of non-alcoholic steatohepatitis. Cells 11 (4), 720.
Naftalin, R.J., 2016. A computer model simulating human glucose absorption and metabolism in health and metabolic disease states. F1000Research 5.
Nain-Perez, A., Füchtbauer, A.F., Håversen, L., Lulla, A., Gao, C., Matic, J., Monjas, L., Rodríguez, A., Brear, P., Kim, W., 2022. Anthraquinone derivatives as ADP-competitive inhibitors of liver pyruvate kinase. Eur. J. Med. Chem. 234, 114270.
Netti, P.A., Baxter, L.T., Boucher, Y., Skalak, R., Jain, R.K., 1997. Macro-and microscopic fluid transport in living tissues: Application to solid tumors. AIChE J. 43, 818–834.
Nomura, K., Yamanouchi, T., 2012. The role of fructose-enriched diets in mechanisms of nonalcoholic fatty liver disease. J. Nutr. Biochem. 23, 203–208.
Ohno, K.I., Tachikawa, K., Manz, A., 2008. Microfluidics: applications for analytical purposes in chemistry and biochemistry. Electrophoresis 29, 4443–4453.
Padole, P., Arora, A., Sharma, P., Chand, P., Verma, N., Kumar, A., 2022. Saroglitazar for nonalcoholic fatty liver disease: a single centre experience in 91 patients. J. Clin. Experimental Hepatol. 12, 435–439.
Parker, R.S., Clermont, G., 2010. Systems engineering medicine: engineering the inflammation response to infectious and traumatic challenges. J. R. Soc. Interface 7, 989–1013.
Peppas, N.A., Langer, R., 2004. Origins and development of biomedical engineering within chemical engineering. AIChE J. 50, 536–546.
Petäjä, E.M., Yki-Järvinen, H., 2016. Definitions of normal liver fat and the association of insulin sensitivity with acquired and genetic NAFLD—a systematic review. Int. J. Mol. Sci. 17, 633.
Petta, S., Valenti, L., Bugianesi, E., Targher, G., Bellentani, S., Bonino, F., Ferrannini, E., Loguercio, C., Lonardo, A., Marra, F., 2016. A "systems medicine" approach to the study of non-alcoholic fatty liver disease. Digestive Liver Dis. 48, 333–342.
Roglans, N., Vila, L., Farré, M., Alegret, M., Sánchez, R.M., Vázquez-Carrera, M., Laguna, J.C., 2007. Impairment of hepatic Stat-3 activation and reduction of PPARα activity in fructose-fed rats. Hepatology 45, 778–788.
Roncal-Jimenez, C.A., Lanaspa, M.A., Rivard, C.J., Nakagawa, T., Sanchez-Lozada, L.G., Jalal, D., Andres-Hernando, A., Tanabe, K., Madero, M., Li, N., 2011. Sucrose

induces fatty liver and pancreatic inflammation in male breeder rats independent of excess energy intake. Metabolism 60, 1259–1270.
Ryoo, J.H., Suh, Y.J., Shin, H.C., Cho, Y.K., Choi, J.M., Park, S.K., 2014. Clinical association between non-alcoholic fatty liver disease and the development of hypertension. J. Gastroenterol. Hepatol. 29, 1926–1931.
Santoleri, D., Titchenell, P.M., 2019. Resolving the paradox of hepatic insulin resistance. Cellular Mol. Gastroenterol. Hepatol. 7, 447–456.
Schmilovitz-Weiss, H., Hochhauser, E., Cohen, M., Chepurko, Y., Yitzhaki, S., Grossman, E., Leibowitz, A., Ackerman, Z., Ben-Ari, Z., 2013. Rosiglitazone and bezafibrate modulate gene expression in a rat model of non-alcoholic fatty liver disease-A historical prospective. Lipids Health Dis. 12, 41.
Schultz, A., Barbosa-Da-silva, S., Aguila, M.B., Mandarim-De-lacerda, C.A., 2015. Differences and similarities in hepatic lipogenesis, gluconeogenesis and oxidative imbalance in mice fed diets rich in fructose or sucrose. Food Funct. 6, 1684–1691.
Sharp, P., Hockfield, S., 2017. Convergence: the future of health. Science 355, 589.
Sherwood, L., 2015. Human physiology: from cells to systems. Cengage learning.
Stanhope, K.L., Griffen, S.C., Bair, B.R., Swarbrick, M.M., Keim, N.L., Havel, P.J., 2008. Twenty-four-hour endocrine and metabolic profiles following consumption of high-fructose corn syrup-, sucrose-, fructose-, and glucose-sweetened beverages with meals. Am. J. Clin. Nutr. 87, 1194–1203.
Stanhope, K.L., Schwarz, J.M., Keim, N.L., Griffen, S.C., Bremer, A.A., Graham, J.L., Hatcher, B., Cox, C.L., Dyachenko, A., Zhang, W., 2009. Consuming fructose-sweetened, not glucose-sweetened, beverages increases visceral adiposity and lipids and decreases insulin sensitivity in overweight/obese humans. J. Clin. Investig. 119, 1322–1334.
Tiersma, J.F., Evers, B., Bakker, B.M., Jalving, M., de Jong, S., 2022. Pyruvate dehydrogenase kinase inhibition by dichloroacetate in melanoma cells unveils metabolic vulnerabilities. Int. J. Mol. Sci. 23, 3745.
Vodovotz, Y., An, G., Androulakis, I.P., 2013. A systems engineering perspective on homeostasis and disease. Front. Bioeng. Biotechnol. 1, 6.
Worthington, C.C., 1988. Worthington enzyme manual: enzymes and related biochemicals. Worthington Biochemical Corporation.
Yin, J., 2007. Chemical engineering and virology: challenges and opportunities at the interface. AIChE J. 53, 2202–2209.